Vibrational Properties and Lateral Interactions of the (2×2)-(O+CO) Coadsorbate Layer on Ru(001)†

K. L. Kostov,‡ W. Widdra,§ and D. Menzel*

Physik-Department E20, Technische Universität München, D-85748 Garching, Germany

Received: January 30, 2004; In Final Form: April 1, 2004

Using highly resolved electron energy loss spectroscopy, we have investigated the (2×2)-(O+CO) coadsorbate layer on Ru(001). All adsorbate-derived modes have been determined. CO-derived modes at 56, 411, 462, and 2048 cm^{-1} are found for the frustrated translation parallel to the surface, the frustrated translation perpendicular to the surface, the frustrated rotation, and the internal C−O stretch mode, respectively, at the Γ point. The oxygen vibrations within the (2×2) coadsorbate structure are found at 431 and 525 cm^{-1} for the Ru−O bending and stretching vibrations, respectively. Off-specular data reveal a dispersion of the internal CO and the Ru−O stretching vibrations due to dynamical dipole−dipole interactions; the other modes are dispersionless within our detection limits. Overtone and combination modes are detected and assigned. The details of the frustrated translation parallel to the surface and its overtone are compared to data for the (√3×√3)-CO layer and discussed with respect to a previously proposed tilting of the molecular axis in the (2×2)-(O+CO) layer. A proposal is made to resolve apparent disagreement between earlier quantitative low-energy electron diffraction measurements and density functional theory calculations.

1. Introduction

Coadsorption can be a step preceding reaction between adsorbates on surfaces. But even in unreactive cases the study of the properties of coadsorbates is very helpful for the understanding of the interactions between different adspecies; in fact, such cases can make an understanding of basic lateral interactions easier, because the absence of reactive steps allows a cleaner analysis. Publications from this group have in the past studied a number of coadsorption systems of simple atoms and molecules on the close-packed Ru(001) surface (as in many preceding publications, we use the nonredundant three-digit notation also for hexagonal crystals) and have determined their geometries (for a compilation, see ref 1), their electronic and vibrational properties,[2−8] and the changes of binding energies and adsorption−desorption kinetics[2,7−9] induced by the adsorbate−adsorbate interactions. We have also addressed questions related to the possible influence of coadsorbates on the spectroscopic properties of a certain adspecies which are a consequence of the method rather than the chemistry, and which have to be understood for reliable interpretations of spectroscopic data. For instance, in vibrational spectroscopies of O + NO layers the chemical shift due to neighboring and next-nearest neighbor atoms and molecules as well as the lateral dynamical coupling could be identified and clearly separated.[10−12]

One of the interesting nonreactive coadsorbate pairs on this surface is that of atomic oxygen and CO. Originally of interest because of the CO oxidation reaction, it turned out that the uncorroded Ru(001) surface is a very poor mediator of this reaction,[2,13] even up to monolayer coverage.[14] A number of well-defined coadsorbate systems exist which have been characterized by quantitative low-energy electron diffraction (LEED), temperature-programmed desorption (TPD) spectroscopy, and vibrational spectra.[3,4,6,8,15] These systems have gained additional interest by the detailed theoretical investigations with large-scale density functional theory (DFT) calculations by Scheffler and co-workers.[16−25] In general the agreement between experiment and theory has been very good for the monosystems, in particular for the sequence of structures formed by atomic oxygen; here their theoretical work[16,17] was decisive for the search for and discovery of high-coverage[17,26] and oxidic structures.[14] In a very successful interplay of experiment and theory, the formation of well-defined surface oxides with specific active sites has been shown to be the prerequisite of fast reaction,[14,23,24] while no coverage range was found in which the CO oxidation would be fast on the unmodified surface.

Nevertheless, the unreactive coadsorbate structures are good model systems for the study of interaction effects. The simplest and most open (O+CO) structure on Ru(001) is the (2×2)-(O+CO) structure. In it the oxygen atoms occupy their normal hcp sites in the (2×2) mesh, and an equal number of CO molecules sit on their preferred on-top site[4] in the center of three O atoms. The LEED determination showed that the (2×2)-O geometry is essentially unchanged by the presence of the CO molecules, while the CO molecules are noticeably influenced. The Ru−CO bond is weaker in this situation compared to that of the √3 structure of pure CO (in which the CO−CO distance is somewhat smaller than the CO−O distance here),[3] and the internal stretch frequency is a bit larger.[27] While there are weak attractive CO−CO interactions in the √3 CO layer,[28] there is now a dominant repulsive interaction between CO and O. Using helium atom scattering (HAS), the low-energy vibrations of this mixed layer as well as those of the pure CO layer at various coverages have been investigated;[7] the results of this work will be used below for comparison where possible.

The LEED results for the (2×2)-(O+CO) structure had one peculiar feature: distinctly the best agreement of measured and

† Part of the special issue "Gerhard Ertl Festschrift".

‡ Permanent address: Institute of General and Inorganic Chemistry, Bulgarian Academy of Sciences, 1113 Sofia, Bulgaria.

§ Max-Born-Institut, Berlin, Germany. New address: Exp. Physik III, Martin-Luther-Universität Halle-Wittenberg, D-06099 Halle, Germany.

10.1021/jp049573e CCC: $27.50
Published on Web 05/26/2004

calculated IV curves was found if the C_{3v} symmetry of the system was broken and the CO axis was given a tilt of about 13°.[4] This was explained by the asymmetric action of the O−CO repulsion in the [1,−1,0] planes (3-fold symmetrically repeated), which is mediated by field-induced orbital rearrangements of the adsorbed CO.[4,29] A subsequent temperature-dependent LEED study using analyses with split positions as well as with a scheme based on probability density functions permitting anisotropic vibrations,[30] which also compared the coadsorbate situation to that in the $\sqrt{3}$ CO layer, corroborated that in the mixed layer there is a static tilt upon which a growing dynamic angular displacement is superimposed if the temperature is increased. Compared to the $\sqrt{3}$ CO (no static tilt, rather soft potential against parallel displacement), the CO with the three O neighbors felt a harder potential for parallel shifts, in particular toward the O neighbors, i.e., in the direction counteracting the static tilt.

The theoretical investigation of Stampfl et al.[18,21] generally found good agreement with these experimental results. The only point of difference was related to the described static tilt, which was not found. Their results were at most compatible with a dynamic tilt on the order of 6° which would derive from a rather flat angular potential around the surface normal.

In the present paper we report a high-resolution electron energy loss (HREELS) study of the vibrational properties of this layer with increased resolution (1−3 meV). Even though HAS on one hand and infrared reflection−absorption spectroscopy (IRAS) on the other have higher resolution, the advantage of this method is that the entire range of vibrational excitations, including multiple losses, can be accessed with the same method on the same sample, and that HREELS makes it possible to also measure the vibrational structure in the entire *k*-space and—compared to IRAS—to detect nondipole excitations. We also study in detail multiple losses in this system. These results shed light on the lateral interactions of the adsorbed species. It was hoped also to obtain additional information on the question of the possible tilt of the CO under the asymmetric repulsive influence of its oxygen neighbors.

2. Experimental Section

The HREELS experiments reported here were performed in a two-chamber ultra-high-vacuum (UHV) system (base pressure $<5 \times 10^{-11}$ mbar) described previously.[10] Briefly, it is equipped with standard four-grid LEED optics, a quadrupole mass spectrometer, an Ar^+ ion sputter gun, work-function facilities, an X-ray source and a hemispherical analyzer for X-ray photoelectron spectroscopy (XPS), and an HREEL spectrometer. For the purposes of the present study mainly the HREEL spectrometer (Delta 0.5, VSI) has been used. At low electron energies (4 eV) the usable resolution of the spectrometer is about 1 meV (8 cm^{-1}) for specular measurements, at an elastic peak intensity of more than 10^5 s^{-1}. The dispersion of the vibrational modes has been measured in the $\bar{\Gamma}\bar{K}\bar{M}$ direction of the surface Brillouin zone using electron energies in the range of 4−250 eV and off-specular angles up to 45°. Because of the signal weakness under these conditions, the resolution for the off-specular dispersion measurements was lowered to 2−3 meV.

The Ru sample was cleaned by standard procedures (oxygen adsorption−desorption cycles, final annealing to 1570 K in UHV). The cleanliness of the Ru(001) surface was checked by HREELS. The vibrational spectrum of clean Ru(001) shows only a phonon peak at 253 cm^{-1}, in agreement with previous HAS measurements.[7]

An optimally ordered (2×2)-oxygen layer with an ideal coverage of 0.25 monolayer (ML) (1 ML corresponds to a ratio of 1:1 for the surface Ru atoms to the adsorbate species) was prepared by a stepwise procedure. The first step was exposure to oxygen at a sample temperature of 320 K, followed by annealing to 1250 K to partly desorb the adsorbed oxygen atoms and to ensure an oxygen coverage between 0.25 and 0.5 ML.[2] In the next step the sample was exposed to hydrogen for 5 min at 400 K in front of a microcapillary array, with the chamber pressure rising to 5×10^{-8} mbar. During the hydrogen exposure and for oxygen coverages above 0.25 ML, the oxygen atoms react with hydrogen to form water, which desorbs at this temperature.[31−33] These two steps ensure an oxygen coverage of 0.25 ML, ordered in (2×2) symmetry. Subsequent annealing to 650 K and cooling back leads to significantly improved ordering of this layer.[4] CO molecules were then adsorbed onto the (2×2)-O layer at 90 K. All exposures to oxygen and CO were performed through microcapillary arrays to ensure homogeneous adsorbate layers and low background pressure in the spectrometer chamber during and after adsorption, so that the mixed layers are well ordered and virtually free of impurities. Even then in longer lasting measurements, such as dispersion experiments, some small amounts of impurities could possibly have collected. Therefore, in these cases the (2×2)-(O+CO) layer was annealed up to 360 K after every recorded spectrum, to remove such impurities (mainly water and hydrogen); the good quality of the layer was restored in this way. All vibrational measurements of the annealed coadsorbate O + CO layers were carried out after subsequent cooling to 90 K. Comparison measurements on $\sqrt{3}$ CO were done following preparation procedures described in the literature.[28,34,35]

3. Results and Interpretation

3.1. High-Resolution Vibrational Spectra of (2×2)-O and of Its CO Coadsorbate Layers. The starting point of the study is the optimally ordered (2×2)-O layer. Its vibrational spectrum measured in specular geometry, i.e., at the $\bar{\Gamma}$ point, is shown in Figure 1a. The oxygen adatoms are known to be coordinated in 3-fold hcp sites[36] with C_{3v} symmetry. Therefore, three normal modes can be associated with this adsorbate complex.[37] One of them is dipole active and polarized perpendicular to the surface. The peak at 526 cm^{-1} (Figure 1a) represents this ν(Ru−O) stretching mode.

The other two oxygen-induced modes are degenerate; they correspond to the frustrated motion parallel to the surface.[38,39] The very-low-intensity feature at about 415 cm^{-1} (Figure 1a) is due to them, as is known from off-specular measurements not shown.[40] The weak, broad loss at around 450 cm^{-1} was not reproducible; it is likely due to small traces of water adsorbed from the residual gas at the sample temperature of 90 K.[41] This low-intensity loss peak disappears in off-specular measurements of the (2×2)-ordered oxygen layer, showing that it is due to a dipole-active mode. This is important to note because for the saturated (2×2)-(O+CO) layer a loss at about 460 cm^{-1} is detected in the *off*-specular direction which we will attribute to adsorbed CO. The low-frequency peaks at 148 and 237 cm^{-1} (Figure 1a) represent surface resonance modes which are backfolded from the $\bar{M}$ point of the surface Brillouin zone to its center $\bar{\Gamma}$ in the presence of the (2×2)-oxygen overlayer.[38,39]

Subsequent CO exposure onto this well-ordered (2×2)-O layer up to saturation at 90 K leads to a coadsorbed (O+2CO) layer with two CO molecules per (2×2)-O unit mesh: one at the on-top and one at the 3-fold site.[6] Figure 1b shows the HREEL spectrum of this saturated layer as prepared at 90 K. The on-top and 3-fold CO species are characterized by internal ν(C−O) stretching vibrations at 2060 and 1836 cm^{-1}, respec-

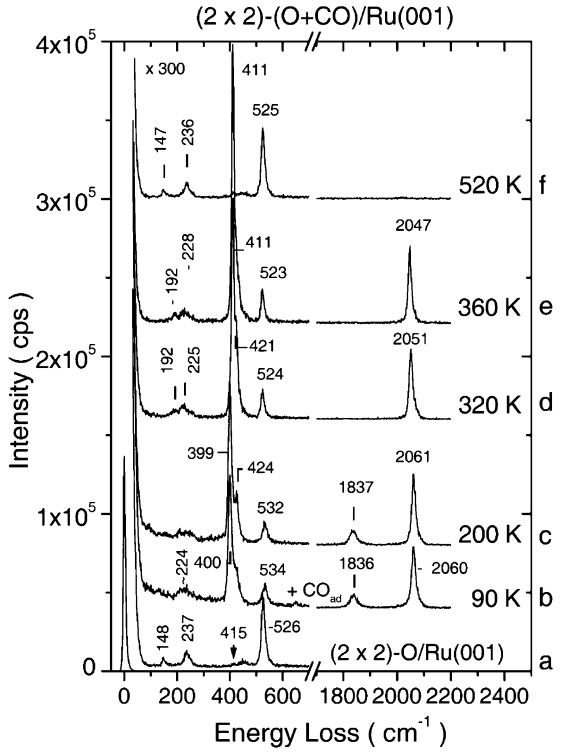

Figure 1. HREEL spectra of adsorbate layers: (a) well-ordered (2×2)-oxygen layer (0.25 ML); (b) subsequent exposure to CO at 90 K. Annealing of the resulting (2O+CO) layer to different temperatures: (c) 200 K; (d) 320 K; (e) 360 K—formation of an optimal (O+CO)-(2×2) layer; (f) 520 K—removal of CO.

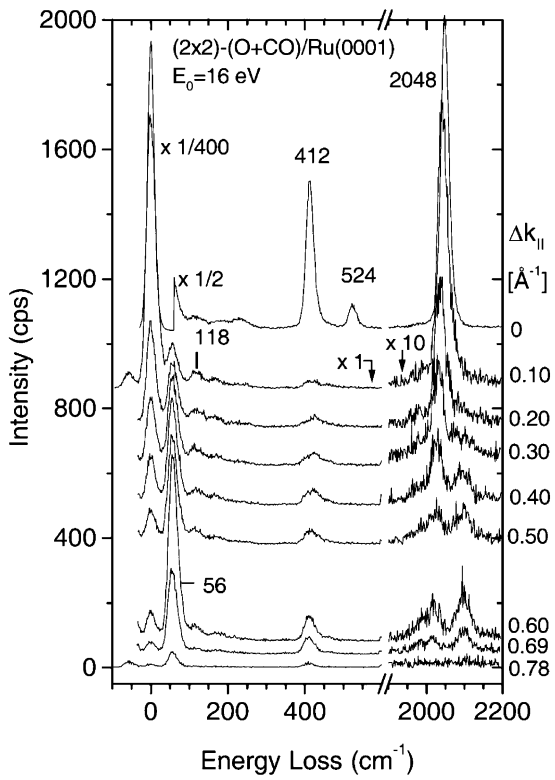

Figure 2. Off-specular HREEL spectra for an electron energy of 16 eV and a fixed total scattering angle of 120°. The corresponding parallel momentum transfer $\Delta k_{||}$ is indicated on the right side.

tively. Their external vibrations perpendicular to the surface are intense and appear at 400 and as a shoulder at ∼420 cm^{-1}, respectively (Figure 1b). The ν(Ru−O) stretching mode undergoes an 8 cm^{-1} upward shift to 534 cm^{-1} compared to that of the pure (2×2)-O layer. Annealing to 200 K conserves the coverage[6] but leads to improved order, as seen by the now clearly resolved external CO−Ru vibrations at 399 and 424 cm^{-1} for the on-top and 3-fold adsorbed CO molecules, respectively (Figure 1c). All 3-fold adsorbed CO molecules are desorbed upon annealing to 320 K (Figure 1d). However, previous studies[3,6] had shown that the resulting (O+CO) coverage is still not optimal, but contains a small amount of additional CO at imperfections of the (2×2)-O layer, most probably at (2×2)-O domain boundaries where the oxygen coverage is locally higher than 0.25 ML. Indeed, in addition to the intense ν(Ru−CO) peak of the on-top CO in the (2×2)-O domains at 411 cm^{-1}, we observe a shoulder of this peak at about 421 cm^{-1} (Figure 1d) showing the presence of a small amount of a second type of linearly adsorbed CO.

Subsequent annealing to 360 K leads to further optimization of the (O+CO)-(2×2) layer with a O:CO ratio of 1:1.[3,4,6] The vibrational spectrum of this layer is shown in Figure 1e. The linearly adsorbed CO is characterized by peaks at 2047 and 411 cm^{-1} attributed to the internal C−O and external CO−Ru stretching modes, respectively. Both values agree well with an earlier FTIR investigation which found 2051 and 412 cm^{-1} upon annealing to 327 K.[6] The oxygen-induced loss at 523 cm^{-1} seems to be uninfluenced by the presence of the coadsorbed CO. This is shown by the vibrational spectrum of the (2×2)-O layer left behind after desorption of the coadsorbed CO molecules (Figure 1f): within experimental error the Ru−O stretching mode does not change its frequency by the removal of CO. In contrast, the two surface phonon modes (at 148 and 237 cm^{-1} for the pure (2×2)-O layer) change their frequencies from 192 and 228 cm^{-1} in the presence of CO to 147 and 236 cm^{-1} after CO removal. The latter is in excellent agreement with the initial O layer (Figure 1a).

The well-ordered (2×2)-(O+CO) layer is the object of our further study. The $\Delta k_{||}$ dependence of its vibrational features will be described next.

3.2. Vibrational Modes of (2×2)-(O+CO)/Ru(001) and Their $\Delta k_{||}$ Dependence: Nondipole Modes and Dispersion. The dispersion of the vibrational modes with surface lattice momentum $k_{||}$ can be inferred from off-specular HREEL spectra. Figure 2 shows such spectra for the well-ordered (2×2)-(O+CO) layer after annealing to 360 K and for parallel momentum transfer $\Delta k_{||}$ between 0 and 0.78 $Å^{-1}$, which correspond to the $\bar{\Gamma}$ and the $\bar{K}'$ points of the (2×2)-surface Brillouin zone, measured with an electron energy of 16 eV. At the $\bar{\Gamma}$ point we obtain almost the same spectrum for the oxygen- and CO-induced vibrations as in the high-resolution measurements at an electron energy of 4 eV (Figure 1). Additionally, a new loss feature is detected around 118 cm^{-1} below the optical surface phonons at ∼190 and 228 cm^{-1}. This peak is more clearly resolved for increasing $\Delta k_{||}$ (as already seen in the second spectrum from the top in Figure 2).

With increasing $\Delta k_{||}$ its energy stays constant at about 112−118 cm^{-1}, indicating a dispersionless feature. Simultaneously another intense loss feature at 56 cm^{-1} grows in with increasing $\Delta k_{||}$ and attains maximum intensity at 0.6 $Å^{-1}$ near the $\bar{K}'$ point (Figure 2). Both new dispersionless modes at 56 and 118 cm^{-1} are not connected with the (2×2)-oxygen overlayer; i.e., they must be due to the CO. According to a previous HAS study of CO and O + CO layers on Ru(001), these new modes have frequencies in the range of frustrated CO translations parallel to the surface.[7]

In the 400−500 cm^{-1} range a broad peak structure is observed in Figure 2 which changes with $\Delta k_{||}$. In this energy loss range

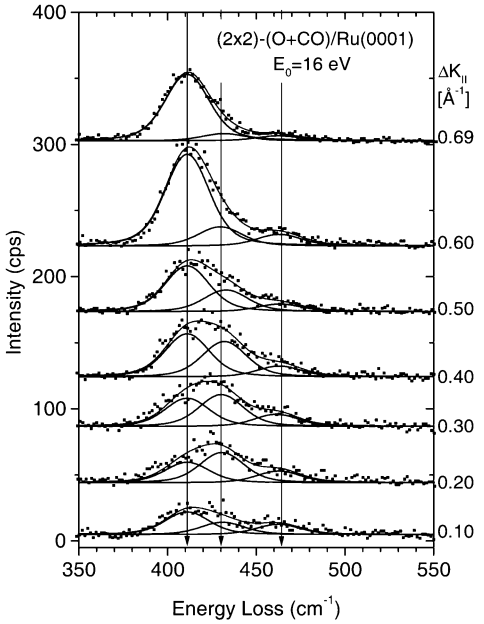

Figure 3. Deconvolution of the external ν(Ru−CO) region for different $\Delta k_{||}$ values (detail of the data of Figure 2).

the frustrated CO translations perpendicular to the surface, the frustrated CO rotations, and the parallel oxygen modes are expected. From the data in specular geometry (Figure 1) the frequency of the dipole-active perpendicular CO translation is known to be 411 cm^{-1} at $\Delta k_{||} = 0$. Deconvolution of these vibrational features is shown in Figure 3.

For $\Delta k_{||} = 0.69$ Å^{-1}, which corresponds to the zone boundary of the (2×2) structure, the spectrum in this energy range is dominated by a single loss peak at 411 cm^{-1}. On the basis of this unshifted frequency, a significant dispersion of the frustrated CO translation perpendicular to the surface is ruled out for this layer. Consequently, for the deconvolution shown in Figure 3 the energy of this mode has been kept constant for all $\Delta k_{||}$ values. The second feature at around 431 cm^{-1} dominates at intermediate momenta and is seen best at $\Delta k_{||} = 0.3$ Å^{-1}. Its spectral position stays constant within the deconvolution uncertainty of 5 cm^{-1}. It is assigned to the Ru−O bending vibration which has been found at 515 cm^{-1} for the (2×2)-O layer on Ru(001).[40]

A third but low-intensity peak is distinguished at about 462 cm^{-1}. Due to its low intensity only an upper limit of 5 cm^{-1} for its dispersion can be given. As the new loss is not observed in the dispersion measurements of the pure (2×2)-oxygen layer on Ru(001),[40] we assign it to a frustrated CO rotation (around an in-plane axis).

Another interesting feature in Figure 2 is found in the range of the ν(C−O) stretching mode at 1950−2100 cm^{-1}. At the $\bar{\Gamma}$ point an intense single peak at 2048 cm^{-1} is observed. Increasing the parallel momentum transfer leads to a downward dispersion of this mode to 2015 cm^{-1} at $\Delta k_{||} = 0.69$ Å^{-1}. Additionally, a second loss feature is observed in the 2080−2100 cm^{-1} range for $\Delta k_{||} > 0.2$ Å^{-1} which is the dominant peak for $\Delta k_{||} = 0.60$ Å^{-1}. A third weak feature is found around 1970−1985 cm^{-1} as shown in Figure 4 in more detail for $\Delta k_{||} = 0.69$ Å^{-1}. Figure 4 shows that these three features can be separated.

Note that the energy separation between the peak at 1985 and the peak at 2098 cm^{-1} amounts to 113 cm^{-1}, which is twice the frequency (2 × 56 cm^{-1}) of the strong loss peak for the frustrated translation parallel to the surface. The intensities of the additional features follow approximately the intensity of the frustrated parallel translation.

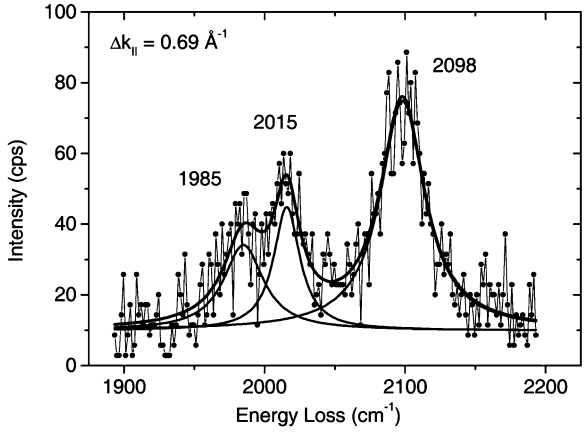

Figure 4. Deconvolution of the internal ν(C−O) region for $\Delta k_{||} = 0.69$ Å^{-1} (detail of the data of Figure 2).

Therefore, the two peaks at 2098 and 1985 cm^{-1} are identified as combination losses due to the dipole-active excitation of the CO stretching mode at 2048 cm^{-1} (at $\Delta k_{||} = 0$) *and* the non-dipole-active excitation (and deexcitation, respectively) of the CO frustrated parallel translation at ±56 cm^{-1} (at $\Delta k_{||} \neq 0$). Whereas in general both modes can contribute to the total momentum transfer, here the CO frustrated parallel translation carries the total momentum since the intensity of the CO stretching mode is strongly peaked at $k_{||} = 0$. This explains nicely that the loss and gain peaks are centered around the frequency of the CO stretching mode seen under dipole scattering conditions and not around the CO stretching mode at $\Delta k_{||} = 0.69$ Å^{-1}, which is visible as the center peak in Figure 4.

Vibrational spectra of the (2×2)-(O+CO)/Ru(001) layer for a larger range of momentum transfers are shown in Figure 5, obtained with electron energies in the range of 32−169 eV.

The second low-energy peak is better resolved here, and its spectral position is refined to 114 cm^{-1}, with no measurable dispersion. For some spectra it is more intense than the 56 cm^{-1} peak. The spectra recorded at the centers $\bar{\Gamma}$ ($\Delta k_{||} = 0$ Å^{-1}) and $\bar{\Gamma}'$ ($\Delta k_{||} = 2.33$ Å^{-1}) of the first and the second surface Brillouin zones (SBZs), respectively, have essentially the same features: distinctly intense elastic peaks and, compared to them, low-intensity vibrational losses. This is additional evidence for the good ordering of the coadsorbate (O+CO) layer with a (2×2) superstructure. In contrast to the low-frequency losses, the weak signal in the ν(C−O) range does not allow an accurate determination of the frequency of the internal C−O stretch under the conditions of Figure 5.

The dispersion measurements from datasets for nine different electron energies in the range from 4 to 250 eV are summarized in Figure 6.

The ν(C−O) mode undergoes a small downward shift from 2048 cm^{-1} at the $\bar{\Gamma}$ point ($\Delta k_{||} = 0$) to 2019 cm^{-1} at $\bar{K}'$ ($\Delta k_{||} = 0.77$ Å^{-1}). In the range from 0.8 to 1.6 Å^{-1} its dispersion is flat. For higher transferred momenta of 1.6−2.3 Å^{-1} which correspond to the $\bar{K}'$ and $\bar{\Gamma}'$ points of the second (2×2) SBZ, the mode disperses upward again to the value found at $\Delta k_{||} = 0$. Note that the mirror symmetric dispersion with respect to the $\bar{M}'$ point (at $\Delta k_{||} = 1.2$ Å^{-1}) which is clearly seen in Figure 6 corroborates that the (2×2)-ordering of the CO is very good. In the same $\Delta k_{||}$ region no significant dispersion is observed for the external ν(Ru−CO) frequency. It changes from 411 to 408 cm^{-1}, which is at the limit of the experimental error for this weak signal. The ν(Ru−O) stretching mode disperses from 525 cm^{-1} at the $\bar{\Gamma}$ point to 511 cm^{-1} at the $\bar{K}'$ point and back

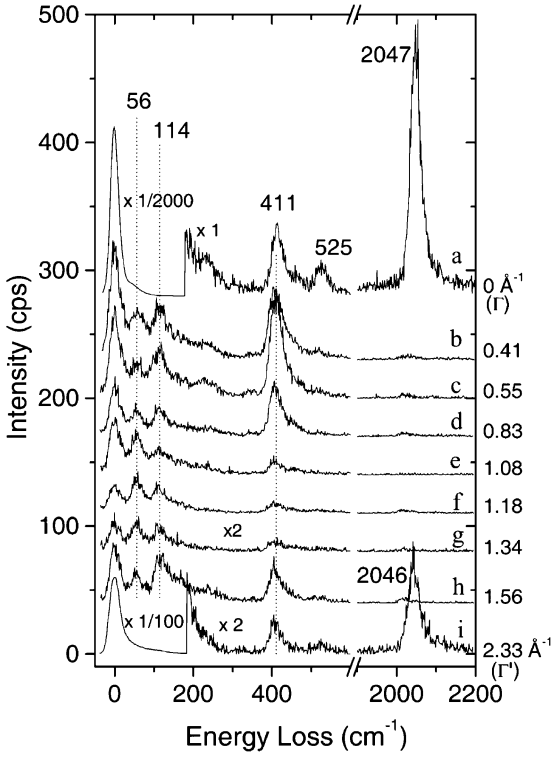

Figure 5. Off-specular HREEL spectra at different $\Delta k_{||}$ values and energies of the incident electrons: 32 eV (b−d); 49 eV (f, g); 81 eV (e); 169 eV (a, h, i).

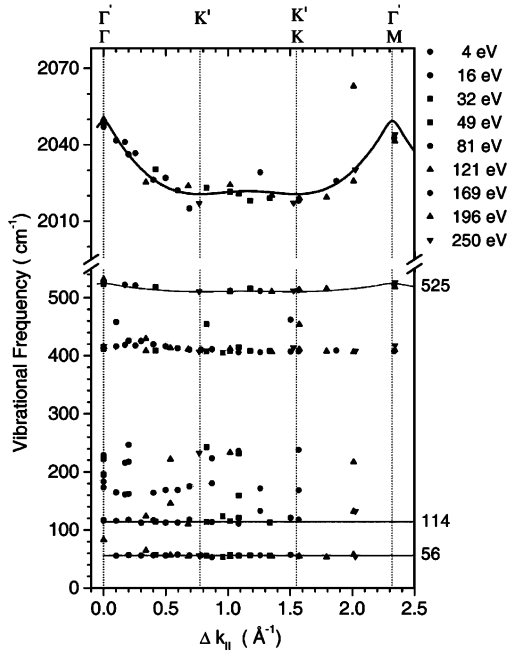

Figure 6. Dispersion curves of the (2×2)-(O+CO)/Ru(001) vibrational modes in the $\overline{\Gamma KM}$ direction of the surface Brillouin zone.

again to 525 cm^{-1} between 1.55 and 2.3 Å^{-1}. Within experimental error this dispersion is the same as that for the pure (2×2)-O layer.[40] It can be explained by a lateral coupling due to dynamical dipole−dipole interactions with identical coupling parameters as have been used successfully for the long-range interaction within the high-density (1×1)-O layer on Ru(001).[42]

For the interpretation of the low-energy CO mode at 114 cm^{-1} a comparison with the well-defined $(\sqrt{3}\times\sqrt{3})R30°$-CO structure will be helpful. Therefore, we show in Figure 7 the off-specular HREEL data for an electron energy of 16 eV as in Figure 2,

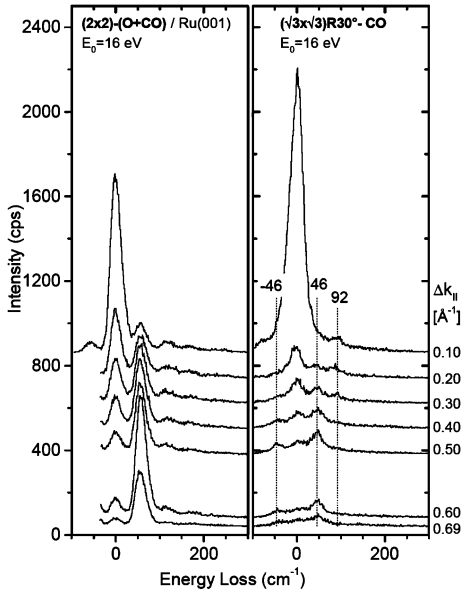

Figure 7. Comparison of off-specular HREEL spectra for the (2×2)-(O+CO) and $(\sqrt{3}\times\sqrt{3})R30°$-CO layers on Ru(001) under identical scattering conditions. The electron energy is 16 eV with a fixed total scattering angle of 120°. The parallel momentum transfer $\Delta k_{||}$ due to the off-specular scattering is indicated on the right side.

together with the same data for $(\sqrt{3}\times\sqrt{3})R30°$-CO measured in the same apparatus under identical conditions.

Two low-energy features are again clearly visible for the $(\sqrt{3}\times\sqrt{3})R30°$ layer at 46 and approximately 92 cm^{-1}. Apart from the shift from 56 and 114 cm^{-1} for the (2×2)-(O+CO) layer, they are equivalent, even though the $\Delta k_{||}$ dependence of the relative intensities is somewhat different. The frequency of the loss peak at 46 cm^{-1} which is accompanied by a corresponding energy gain peak at −46 cm^{-1} agrees well with the helium scattering data for this system.[7]

4. Discussion

Our measurements have given a detailed overview over all vibrational excitations in this coadsorbate system with a single method. Where overlap exists—for the very-low-energy modes with the HAS results of ref 7 and for the high-energy modes with IRAS[6] data—the agreement is very good. In addition to the corroboration of these data—which is important in view of the different selection rules operative in the various methods—we have for the first time detected the frustrated rotation at about 460 cm^{-1}. We have also tested the dispersion for all modes. Only for the modes with strong dynamic dipoles, the internal CO stretch and the perpendicular O vibration, have clear dispersions been found. All other modes are dispersionless within our accuracy. To be sure, the sensitivity for changes decreases with the absolute energy values, so that in particular for the low-energy modes the freedom from dispersion has to be taken with caution. On the other hand, the rather large intermolecular distance of CO − two lattice spacings, i.e., 0.54 nm—would suggest weak coupling if no dipole−dipole coupling is available. An exception could be expected in the low-energy regions where there could be coupling via lattice vibrations. However, the low-energy excitations we see are all situated below the optical surface modes of the substrate. The only substrate vibration in the same range as our "dispersionless" adsorbate modes is the Rayleigh mode, which should cross the frustrated parallel CO translation at about $\Delta k_{||} = 0.3$ Å^{-1}.[7] Neither in these HAS measurements nor in our results is any indication of a coupling-induced effect visible.

The negligible dispersion of most modes also corroborates that we need not expect any effect on multiple excitations by coupling to two-phonon continua.[35,43] We can therefore discuss the double losses and combination bands found as localized phenomena. We have shown in the results that the loss due to the internal vibration of CO has sidebands induced by the frustrated parallel motion, causing gain and loss peaks of the latter on the former. In these combined excitations the main intensity is contributed by the strongly-dipole-active internal vibration, while the momentum transfer is contributed by the low-energy dipole-inactive mode. This can be recognized by the fact that the gain and loss peaks which are spaced by twice the energy of the parallel motion are centered on the all-in-phase internal mode as found for $\Delta k_{||} = 0$, not for the actual spectrum at $\Delta k_{||} = 0.69$ Å^{-1}. This corroborates that the coupled losses are induced sequentially, in either sequence.

In the low-energy region the two losses found at 56 (59 in HAS[7]) and at 112−118 cm^{-1} could be either the single and the double losses (i.e., the sequential, incoherent excitation of two single modes) of the frustrated parallel translation—which would explain their rather exact 1:2 ratio—or the fundamental and first overtone of the same excitation—in which case they would be indicative of a potential very close to harmonic in this range. For dipole scattering the intensity of the incoherent double loss can be estimated from the intensity ratio between the elastic and the single-loss peaks. For impact scattering, the possibility of strong variations of the impact cross section with electron energy and scattering angle might lead to situations where the single loss is suppressed compared to the double loss. However, the high intensity of the 114 cm^{-1} loss, which exceeds the intensity of the 56 cm^{-1} feature for a wide range of different experimental scattering conditions (see Figure 5), renders this alternative assignment less likely. We will come back to this question after considering another aspect.

This excitation is very interesting also in a different connection. As mentioned in the Introduction, there appears to be a disagreement between the conclusions from LEED-IV and temperature-dependent LEED-IV results on one hand,[4,30] which concluded that the CO has a small but definite static tilt away from the closest O coadsorbate, and the DFT-GGA calculations on the other hand, which gave essentially a perpendicular orientation of the CO and could only be reconciled with a small dynamic tilt due to a rather flat potential energy surface (PES) for tilting around the upright position.[18,21] The dynamical properties of such a tilted molecule are interesting in their own right, and we would expect to be able to distinguish between these two models using our results.

Since the static tilting of the molecule corresponds dynamically to a frustrated translation parallel to the surface, the low-lying excitations are obviously important in this context. The frequency of the frustrated translation parallel to the surface of 56 cm^{-1} as determined in this work is consistent with the value of 59 cm^{-1} determined by HAS for this coadsorbate system; it is in the same range as the frequencies of 48, 46, 42, and 65 cm^{-1} found there for isolated CO, ($\sqrt{3}\times\sqrt{3}$)*R*30°-CO, ($2\sqrt{3}\times 2\sqrt{3}$)R30°-CO, and a (2×2)-(2O+CO) honeycomb structure, respectively.[7] On the basis of the absence of dispersion for the frustrated parallel translation, the lateral dynamical interaction between different CO molecules can be ignored and the frequencies reflect directly the curvature of the PES with respect to a static tilt. The comparison shows that in the (2×2)-(O+CO) system this mode is harder by about 20% compared to an isolated CO molecule on the same Ru(001) surface, and even more compared to pure CO layers, in qualitative agreement with the conclusions from the LEED results[4,30] and with the picture of a steeper potential wall caused by the nearby O. Indeed, in the (2×2)-(2O+CO) honeycomb structure, in which the CO is symmetrically surrounded by six O atoms and thus cannot have a static tilt for symmetry reasons, the parallel translation sees an even harder potential. So these aspects are in qualitative accord with the LEED-derived picture.

However, other aspects of our findings do not seem to be. A static tilt of the CO molecules corresponds to a symmetry reduction from C_{3v} to C_s which lifts the degeneracy of the parallel frustrated translations. For these one would expect in this case different frequencies along and perpendicular to the [1,−1,0] tilting direction. However, our data do not contain an indication of a second frustrated translation parallel to the surface, nor of a splitting of the 56 cm^{-1} loss. From the rather narrow line width for the frustrated translation which is close to the instrumental resolution as can be seen best in Figure 2 for $\Delta k_{||} = 0.60$, we estimate that—if any splitting due to the symmetry reduction exists—the two frequencies differ by at most 10% (6 cm^{-1}).

This would be understandable if the two frequencies would differ strongly. Two possibilities are conceivable: the second frequency could be either much larger or much smaller than that at 56−59 cm^{-1}. In the first case the second frequency could be that observed at 114 cm^{-1}, which—because of the very good 1:2 ratio—has been tentatively assigned above to the overtone of the frustrated translation, i.e., the excitation from the ground to the second excited vibrational state. The rather exact frequency ratio would have to be a coincidence then. To check on this and corroborate the overtone assignment for the 114 cm^{-1} feature, we directly compare the low-energy region of off-specular HREELS data for the (2×2)-(O+CO) layer with those for the ($\sqrt{3}\times\sqrt{3}$)*R*30°-CO layer (Figure 7). On the right-hand side of Figure 7 the data for a well-ordered ($\sqrt{3}\times\sqrt{3}$) layer are presented for momentum transfers between 0.1 and 0.69 Å^{-1}; on the left-hand side the data for the (2×2)-(O+CO) layer, which have been measured under identical scattering conditions, are redrawn from Figure 2. For the $\sqrt{3}$ layer the energy loss and gain peaks of the frustrated parallel translation are clearly visible at ±46 cm^{-1}, in agreement with the HAS study.[7] Additionally, a loss feature at 92 cm^{-1}, which is again twice the loss energy of the frustrated parallel translation, is seen for this layer. There is no symmetry breaking for this layer, so this agreement for single and double losses for both layers clearly corroborates the assignment. The good frequency ratio 1:2 in both cases shows that for both cases the curvature of the potential energy curve in the low excitation range must be very close to harmonic. Note that, whereas for dipole scattering overtone excitation is forbidden due to selection rules for a harmonic vibrational potential, impact scattering can excite the overtone transition even for a harmonic oscillator. The different intensities for the two different layers, especially for the fundamental mode, are most likely due to different local CO environments which lead to different multiple-scattering conditions as known from LEED-IV variations.

In the second case the opposite extreme would be realized; i.e., the second frequency is now much *lower* than the 56 cm^{-1} measured. If it becomes sufficiently soft, it could lie inside the "elastic" peak and thus become invisible. To see whether this is conceivable, it is helpful to consider how a tilt of the CO evolves from a nontilted starting situation. By introducing increasing repulsive interactions of the CO molecule with the three surrounding oxygen atoms, the PES with respect to the CO parallel motion (which defines the frequency of the

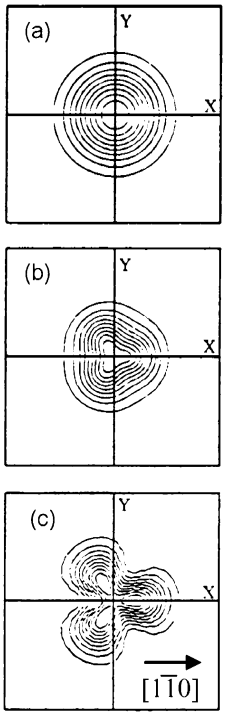

Figure 8. Schematic potential energy surfaces for parallel vibrations with increasing interaction to three equivalent neighbors: (a) no interaction, (b) weak interaction, (c) stronger interactions leading to three shifted minima.

frustrated translation parallel to the surface by the curvatures around its minimum) will be modified. A sequence of three PESs for increasing interaction is sketched schematically in Figure 8.

The CO molecule will oscillate around the *PES minimum*. If for stronger interaction the minimum shifts away from the C_{3v} symmetric on-top site, a local *maximum* will develop at the on-top site as seen in Figure 8c. Consequently, with increasing interactions the curvature of the PES at the on-top site has to change sign. Therefore, one expects with increasing interaction first a mode softening, before the on-top site becomes unstable and three new minima appear (Figures 8b,c). Such mode softening is well-known as a precursor for surface reconstructions.[44] Since the PES always has a horizontal tangent at the on-top C_{3v} symmetric site, any vibration in the plane containing an O neighbor—e.g., the [1,−1,0] direction—will be very soft and highly anharmonic. It is quite conceivable that the vibration toward the center becomes so soft that the corresponding loss is within the width of the "elastic" loss (about 25 cm^{-1}) and therefore cannot be measured. Perpendicular to this direction, however, the change should be smaller, but now in the direction of a hardening of the vibration; in Figure 8c the valley at one of the three minima becomes narrower in the nondisplaced direction. It could then correspond to our measured 56 cm^{-1}. This would also make it understandable that this vibration as well as the corresponding one for the pure CO layer is so close to harmonic. The soft vibration would then be fully excited even at our 90 K, explaining why very little change of displacement has been seen in the low-temperature region in the *T*-dependent LEED results.

This second interpretation of our observations possesses the attractive feature that it leads to a resolution of the apparent disagreements among the LEED, DFT, and present results with respect to the question of the CO tilt. We therefore suggest that the reason for our failure to identify a vibrational loss which can be assigned to the parallel vibration *in* the direction of the tilt is due to its strong softening making it unobservable, and the *observed* loss corresponds to the *high*-frequency vibration of the symmetry-split pair. This picture leads to agreement with the small static tilt found by *T*-dependent LEED; it is also compatible with the DFT calculations which did result in a very soft potential around the surface normal.

5. Summary and Conclusions

The vibrational properties of the (2×2)-(O+CO) layer on Ru(001) have been studied with highly resolved EELS (8−20 cm^{-1}). The layer is characterized by CO-derived vibrations at 56, 114, 411, 462, and 2048 cm^{-1} (at $\bar{\Gamma}$) corresponding to the frustrated translation parallel to the surface, its first overtone, the frustrated translation perpendicular to the surface, the frustrated rotation, and the internal C−O stretch mode, respectively. Additionally, O-derived modes are found at 431 and 525 cm^{-1} for the Ru−O bending and stretching vibrations. The dispersion of the internal C−O stretching vibration has been determined along $\overline{\Gamma KM}$ to the center of the second SBZ. It is well described by dynamical dipole−dipole coupling with a phonon bandwidth of 29 cm^{-1} and a singleton frequency of 2026 cm^{-1}. The Ru−O stretching vibration exhibits a weak dispersion of 14 cm^{-1} which is also consistent with dynamical dipole−dipole coupling and can be described by the same parameters derived before for the high-density (1×1)-O layer. All other adsorbate-derived modes show no measurable dispersions.

The detailed experimental data are compatible with the earlier LEED and *T*-dependent LEED data, which resulted in a static tilt, as well as with the DFT calculations if we assume that the frustrated parallel translation in the direction of the tilt (in the plane of the O neighbor) is too soft to be measurable, and assign the 56 cm^{-1} loss to the surface-parallel motion perpendicular to that plane (both repeated with 3-fold symmetry).

Acknowledgment. K.L.K. thanks his home institution for a leave of absence. This work has been supported by the Fonds der Chemischen Industrie and by a Max Planck Prize to D.M.

References and Notes

(1) Menzel, D. *Surf. Rev. Lett.* **1999**, *6*, 835.
(2) Madey, T. E.; Engelhardt, H. A.; Menzel, D. *Surf. Sci.* **1975**, *48*, 304.
(3) Kostov, K. L.; Rauscher, H.; Menzel, D. *Surf. Sci.* **1992**, *278*, 62.
(4) Narloch, B.; Held, G.; Menzel, D. *Surf. Sci.* **1995**, *340*, 159.
(5) Jakob, P.; Gsell, M.; Menzel, D. *J. Chem. Phys.* **2001**, *114*, 10075.
(6) Schiffer, A.; Jakob, P.; Menzel, D. *Surf. Sci.* **1997**, *389*, 116.
(7) Braun, J.; Kostov, K. L.; Witte, G.; Wöll, C. *J. Chem. Phys.* **1997**, *106*, 8262.
(8) Schiffer, A.; Jakob, P.; Menzel, D. *Surf. Sci.* **2000**, *465*, 198.
(9) Kreuzer, H. J.; Payne, S. H.; Jakob, P.; Menzel, D. *Surf. Sci.* **1999**, *424*, 36.
(10) Kostov, K. L.; Menzel, D.; Widdra, W. *Phys. Rev. B* **2000**, *61*, 16911.
(11) Moritz, T.; Widdra, W. *Phys. Rev. Lett.* **2001**, *86*, 103.
(12) Jakob, P. *Surf. Sci.* **1999**, *428*, 309.
(13) Lee, H. I.; White, J. M. *J. Catal.* **1980**, *63*, 261. Boettcher, A.; et al. *Surf. Sci.* **2000**, *466*, L811. Zang, L.; Kisch, H. *Angew. Chem.* **2000**, *112*, 4075.
(14) Over, H.; Kim, Y. D.; Seitsonen, A. P.; Wendt, S.; Lundgren, E.; Schmid, M.; Varga, P.; Morgante, A.; Ertl, G. *Science* **2000**, *287*, 1474.
(15) Narloch, B.; Held, G.; Menzel, D. *Surf. Sci.* **1994**, *317*, 131.
(16) Stampfl, C.; Scheffler, M. *Phys. Rev. B: Condens. Matter* **1996**, *54*, 2868.
(17) Stampfl, C.; Schwegmann, S.; Over, H.; Scheffler, M.; Ertl, G. *Phys. Rev. Lett.* **1996**, *77*, 3371.
(18) Stampfl, C.; Scheffler, M. *Isr. J. Chem.* **1998**, *38*, 409.

(19) Stampfl, C.; Kreuzer, H. J.; Payne, S. H.; Pfnür, H.; Scheffler, M. *Phys. Rev. Lett.* **1999**, *83*, 2993.
(20) Reuter, K.; Scheffler, M. *Surf. Sci.* **2001**, *490*, 20.
(21) Stampfl, C.; Scheffler, M. *Phys. Rev. B* **2002**, *65*, 155417.
(22) Reuter, K.; Scheffler, M. *Phys. Rev. B* **2002**, *65*, 035406.
(23) Reuter, K.; Ganduglia-Pirovano, M. V.; Stampfl, C.; Scheffler, M. *Phys. Rev. B* **2002**, *65*, 165403.
(24) Reuter, K.; Stampfl, C.; Ganduglia-Pirovano, M. V.; Scheffler, M. *Chem. Phys. Lett.* **2002**, *352*, 311.
(25) Reuter, K.; Scheffler, M. *Phys. Rev. B* **2003**, *68*.
(26) Kostov, K. L.; Gsell, M.; Jakob, P.; Moritz, T.; Widdra, W.; Menzel, D. *Surf. Sci.* **1997**, *394*, L138.
(27) Jakob, P. *Physica D* **1998**, *119*, 109.
(28) Pfnür, H.; Menzel, D. *Surf. Sci.* **1984**, *148*, 411.
(29) Wang, R. L. C.; Kreuzer, H. J.; Menzel, D. *Z. Phys. Chem. (Muenchen)* **1997**, *202*, 205.
(30) Landskron, J.; Moritz, W.; Narloch, B.; Held, G.; Menzel, D. *Surf. Sci.* **1999**, *441*, 91.
(31) Shi, S.-K.; Schreifels, J. A.; White, J. M. *Surf. Sci.* **1981**, *105*, 1.
(32) Koch, M. H.; Jakob, P.; Menzel, D. *Surf. Sci.* **1996**, *367*, 293.
(33) Hrbek, J. *J. Phys. Chem.* **1986**, *90*, 6217.
(34) Michalk, G.; Moritz, W.; Pfnür, H.; Menzel, D. *Surf. Sci.* **1983**, *129*, 92.
(35) Jakob, P.; Persson, B. N. J. *J. Chem. Phys.* **1998**, *109*, 8641.
(36) Lindroos, M.; Pfnür, H.; Held, G.; Menzel, D. *Surf. Sci.* **1989**, *222*, 451.
(37) Ibach, H.; Mills, D. L. *Electron Energy Loss Spectroscopy and Surface Vibrations*; Academic Press: New York, 1982.
(38) Rahman, T. S.; Anton, A. B.; Avery, N. R.; Weinberg, W. H. *Phys. Rev. Lett.* **1983**, *51*, 1979.
(39) Mitchell, W. J.; Wang, Y. Q.; Schick, M.; Weinberg, W. H. *J. Chem. Phys.* **1995**, *102*, 8185.
(40) Moritz, T. *Schwingungsspektroskopie an Adsorbatschichten auf der Ru(001)-Oberfläche*; Technische Universität München: Garching, Germany, 2003.
(41) Thiel, P. A.; Hoffmann, F. M.; Weinberg, W. H. *J. Chem. Phys.* **1981**, *75*, 5556.
(42) Moritz, T.; Menzel, D.; Widdra, W. *Surf. Sci.* **1999**, *428*, 64.
(43) Jakob, P.; Persson, B. N. J. *Phys. Rev. B: Condens. Matter* **1997**, *56*, 10644.
(44) Voigtländer, B.; Lehwald, S.; Ibach, H. *Surf. Sci.* **1989**, *208*, 113.